DESIGN OF OPTIMIZED FIXED-POINT WCDMA RECEIVER

Hai-Nam Nguyen, Daniel Menard, and Olivier Sentieys

IRISA/INRIA, University of Rennes 1,
6 rue de Kerampont
F-22300 Lannion
Email: hanguyen@irisa.fr

ABSTRACT

To satisfy energy and complexity constraints, embedded wireless systems require fixed-point arithmetic implementation. To optimize the fixed-point specification, existing approaches are based on fixed-point simulations to evaluate the performances. In this paper, the approach used to optimize the fixed-point specification for a WCDMA receiver is presented. The dynamic range and the fixed-point accuracy are evaluated analytically in our approach. The analytical accuracy constraint expression according to the bit error rate (BER) is proposed. The results show that the optimized fixed-point specification depends on the input receiver signal-to-noise ratio (SNR).

1. INTRODUCTION

Wireless communication is one of the most important sectors for digital signal processing (DSP) applications [12]. The low cost and low power terminal design is one of the key challenges in this domain. New services, such as image, video and Internet access require higher data rate. Consequently, the complexity of the baseband digital part is growing. Different aspects have to be considered to optimize the implementation cost and the power consumption. Especially, the arithmetic aspects offer opportunities to reduce the cost and the power consumption.

Efficient embedded wireless system implementation requires the use of fixed-point arithmetic. Therefore, the vast majority of embedded DSP applications is implemented in fixed-point architectures [2, 3, 11]. Indeed, fixed-point architectures are cheaper and more energy efficient than floating-point architectures because of their lower data word-lengths.

The fixed-point conversion process is made up of two main steps corresponding to the dynamic range estimation and the fixed-point data word-length optimization. The aim of this optimization process is to minimize the implementation cost as long as the application performances are fulfilled. To optimize the fixed-point specification, existing approaches [14, 4] are based on fixed-point simulations to evaluate the performances. In [10], the fixed-point error is analyzed for a CDMA receiver, but the performances in terms of bit error rate is also measured with fixed-point simulations. To evaluate accurately the bit error rate, a great number of samples are needed. Each modification of the fixed-point data requires a new fixed-point simulation. Thus these approaches suffer from a major drawback which is the long optimization time. Consequently, the fixed-point design space cannot be explored and multiple word-length approaches [5] cannot be used.

In this paper the approach used to optimize the fixed-point specification is presented for the case of a WCDMA receiver. The WCDMA technology is used for the physical layer of the Universal Mobile Telecommunications System (UMTS), one of the third generation wireless communication systems. A new approach is proposed to estimate more accurately the data dynamic range. The properties of the application are taken into account to reduce the pessimistic effects of classical analytical approaches like interval arithmetic. Then, the accuracy constraint used in the fixed-point optimization problem is determined from the required application performances. For the bit error rate, the analytical expression of the accuracy constraint according to the bit error rate is proposed. The experiment results show the opportunity to code the fixed-point data according to the receiver signal-to-noise ratio. Our approach can be easily adapted to any communication system.

The paper is organized as follows. In Section 2, the fixed-point conversion process is summarized and the WCDMA receiver is described in Section 3. The design of the symbol decoder module is detailed in Section 4. First, the dynamic range estimation is presented and secondly, the fixed-point specification optimization is described. In Section 5, the design of the searcher module is presented.

2. FIXED-POINT CONVERSION

The fixed-point conversion can be divided into two main steps corresponding to binary-point position determination and word-length optimization. The first step corresponds to the determination of the integer word-length of each datum. The number of bits iwl_i for this integer part must allow the representation of all the values taken by the data, and is obtained from the data bound. Thus, firstly the dynamic range is evaluated for each datum. Then, these results are used to determine, for each datum, the binary-point position which minimizes the integer word-length and which avoids overflow. Moreover, scaling operations are inserted in the application to adapt the fixed-point format of a datum to its dynamic range or to align the binary-point of the addition inputs.

The second step corresponds to the determination of the fractional word-length. The number of bits fwl_i for this fractional part defines the computational accuracy, which is usually measured by the output quantization noise power P_{e_q}. The implementation cost is minimized under the accuracy constraint $P_{e_q}^{\max}$. Let $\mathbf{wl}$ be an N-size vector representing the N application data word-lengths. Let $C(\mathbf{wl})$ be the implementation cost and $P_{e_q}(\mathbf{wl})$ be the computational accuracy obtained for the word-length vector $\mathbf{wl}$. The implementation cost $C(\mathbf{wl})$ is minimized under the accuracy constraint $P_{e_q}^{\max}$:

$$\min\left(C\left(\mathbf{wl}\right)\right) \qquad \text{such as} \qquad P_{e_q}(\mathbf{wl}) \leq P_{e_q}^{\max} \tag{1}$$

To obtain reasonable optimization times, an analytical approach is used to evaluate the fixed-point accuracy. Moreover, in a wireless communication system, the performance is measured by the error rate. Therefore a relation between the application performance and the accuracy constraint must be done. An analytical expression of the maximal quantization noise power according to the bit error rate at the Rake receiver output is proposed.

3. PRESENTATION OF WCDMA

WCDMA is the air interface of 3G mobile telecommunications networks, which is based on DS-CDMA (Direct Spread Code Division Multiple Access) technology. In WCDMA, two layers of spreading codes are used [13]: channelization codes and scrambling codes. The channelization codes C_{ch} are based on the Orthogonal Variable Spreading Factor (OVSF) technique to allow the change of spreading factor and to maintain the orthogonality between different spreading codes of different lengths. The scrambling codes used

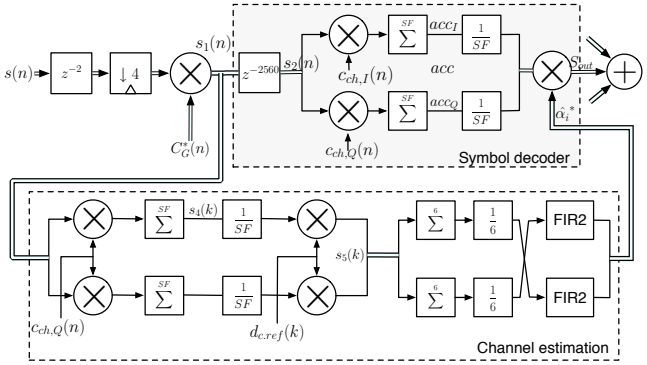

Figure 1: Data flow graph of the i^{th} finger of the WCDMA Rake receiver.

in downlink are long Gold codes C_G. The input data d_t is multiplied with the spreading codes, and the transmitted signal Tx_t is equal to $\mathrm{Tx}_t = d_t C_{ch} C_G$. In a multi-path Rayleigh channel, the global received signal $s(n)$ is the sum of elementary signal $s^i_{in}(n)$ for different channel paths. Let τ_i and α_i be respectively the delay and the complex amplitude of i^{th} path in the channel. The global received signal $s(n)$ expression is equal to

$$s(n) = \sum_i^{N_p} \left(s^i_{in}(n) + n_{in}(n) \right) = \sum_i^{N_p} (\alpha_i \mathrm{Tx}(n-\tau_i) + n_{in}(n)) \qquad (2)$$

The term $n_{in}(n)$ represents the noise term made up of the receiver thermal noise and the interference of the other users. This term can be considered gaussian with variance $\sigma^2_{n_{in}}$. Assuming that a user has one DPDCH channel, $d_t C_{ch}$ take values in $\{\pm 1 \pm i\}$. Thus $\mathrm{Tx} \in \{\pm 2, \pm 2i\}$. For simplification, Tx is normalized into $\{\pm 1, \pm i\}$, hence its power is equal to one. By definition, the signal-to-noise ratio is equal to $\mathrm{SNR} = 1/\sigma^2_{n_{in}}$.

For the WCDMA receiver, the symbol decoding is carried out by a Rake receiver to benefit from the multi-path fading effects. The Rake receiver concept is based on the combination of the different multi-path components in order to improve the quality of symbol decision. Each multi-path signal is assigned to a finger which correlates the received signal by the spreading code shifted with a delay τ_i. Demodulation results from a weighted decision at the correlator outputs. Using the maximum likelihood criteria, the symbol is estimated from the $y(k)$ signal:

$$y(k) = \sum_{i=1}^{N_p} y_i(k) = \sum_{i=1}^{N_p} \alpha_i^*(k) r_i(k) \qquad (3)$$

Thus, the finger is made up of two main parts corresponding to the decoding symbol module and the channel estimation module. The data flow graph of a finger is presented in Figure 1. The complex amplitude α_i of the i^{th} path is estimated by the pilot sequence located in the control frame (DPCCH). Thanks to the complex multiplication of the received signal by the conjugate Gold code, the unscrambling operation is performed. Then, the despreading operation from channelization code transforms the received wide-band signal into a narrow-band signal. Finally, the estimated phase distortion resulting of the transmission channel is removed.

Each finger requires the knowledge of the i^{th} path delay τ_i to obtain the maximal correlation. First, the coarse time delay estimation is carried out with the path searcher. Then, the fine synchronization of the code and the received signal is made with a Delay-Locked Loop (DLL). The data flow graph of the path searcher is presented in Figure 2. The received signal is multiplied by different shifted versions of the spreading codes. A threshold is calculated on the average power, then peaks are determined. Each peak gives potentially a path component according to that shifted time.

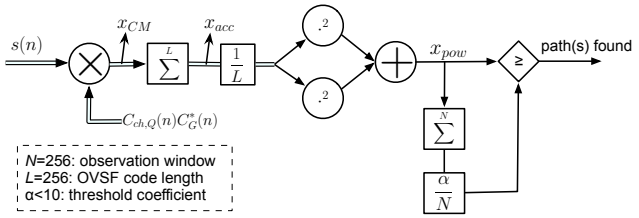

Figure 2: Data flow graph of the path searcher.

4. SYMBOL DECODER

4.1 Dynamic range estimation

The first step of the fixed-point conversion process corresponds to integer word-length determination. It is required to determine each data dynamic range in this step. An analytical approach based on interval arithmetic [6] is used to estimate the dynamic and to guarantee no overflow. However, this method sometimes overestimates the dynamic range if the application properties are not taken into account.

In a direct sequence spead-spectrum system, the signal-to-noise ratio is particularly low. With tens of simultaneous users in communications, the noise and interference power is tens of times higher than the useful signal. The dynamic range is mainly due to the noise and interference. In the despreading process, the signal is summed up over the length L of spreading sequence. The pure analytical approach will multiply the dynamic range by L. But in fact, this process multiplies mainly the dynamic range of useful signal, not that of noise and interference. From this property, an approach is then proposed to determine more accurately the data dynamic range. Before the despreading/correlation process, the whole useful signal plus noise is considered. After this process, only the useful signal is taken into account when calculating the dynamic range.

The dynamic range of different data is computed from the Rake receiver flow graph presented in Figure 1. The input $s(n)$ consisting of desired signal $s^i_{in}(n)$ plus noise $n_{in}(n)$ is normalized to have the maximum amplitude one. Because a gaussian noise $\sigma^2_{n_{in}}$ has 99.7% of its values in $[-3\sigma_{n_{in}}, 3\sigma_{n_{in}}]$, assuming the real and imaginary parts of $s^i_{in}(n)$ are in the interval $[-1,1]$, the input is considered to be in $[-1-3\sigma_{n_{in}}, 1+3\sigma_{n_{in}}]$. The normalization process corresponds to the division of the input by $1+3\sigma_{n_{in}}$.

By propagating the input range in the flow graph, the following results are obtained. The dynamic range of the accumulator output acc_I before normalization is equal to

$$\max(|acc_I|) = \frac{4.SF}{1+3\sigma_{n_{in}}} \qquad (4)$$

The dynamic range of α_i corresponding to the channel estimation module output is equal to

$$\max(|\alpha_i|) = \frac{1}{1+3\sigma_{n_{in}}} \qquad (5)$$

The dynamic range of s_{out} corresponding to the symbol estimation module module is equal to

$$\max(|s_{out}|) = \frac{4}{(1+3\sigma_{n_{in}})^2} \qquad (6)$$

The dynamic range has been estimated with our analytical approach for different SNR values and compared with results obtained from simulations. The results are presented in Figure 3 for the accumulator output (acc_I) and for the symbol decoding output (s_{out}). It is noticed that from one to two bits differ between estimated and simulated results. Nevertheless, the dynamic range evolutions according to the signal-to-noise ratio are identical for analytical and

simulation based estimations. This confirms the validity of our approach to estimate the dynamic range in the WCDMA receiver. The difference between the two lines can be explained by the channel model used in the simulation. If a single path channel model, for example, is used, the difference is less than 1 bit. Moreover, the analytical estimations are known to be more pessimistic. For the accumulation output, in both simulation and estimation, there is a difference of 3 bits between 0 dB and 25 dB. For the finger output, there is a difference of 4 bits between 0 dB and 15 dB and of 6 bits between 0 dB and 25 dB. These results show the opportunity to adapt the data integer word-length according to the signal-to-noise ratio at the receiver input.

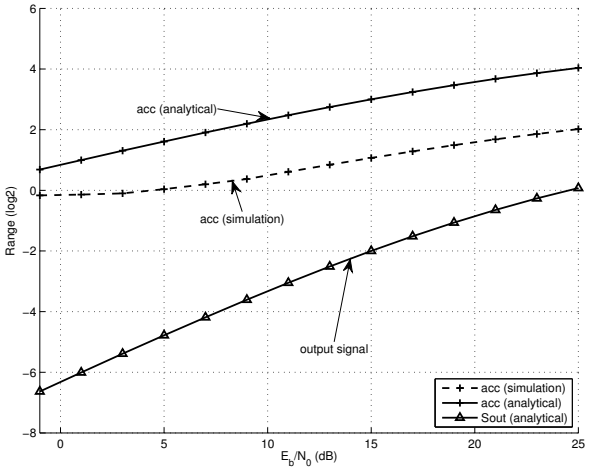

Figure 3: Estimated and simulation based values of dynamic range for the decoder.

4.2 Word-length optimization

In fixed-point implementation, a minimal computation accuracy must be provided to guarantee that the system performances are maintained. For the symbol decoding module as well as the whole system, the performances are evaluated with the bit error rate so that the use of finite precision does not modify the referenced infinite precision (BER_0) more than ε. Suppose that the quantization noise power is P_{e_q}, the performance criterion can be written as:

$$\mathrm{BER}_0 \leq \mathrm{BER}_{P_{e_q}} \leq (1+\varepsilon)\mathrm{BER}_0 \tag{7}$$

4.2.1 Accuracy constraint

Noise model The quantization noise can be modeled by a sum of different noise sources propagating throughout the system. This sum can be considered as a single noise source $\widetilde{e_q}$ at the system output. In [8], this noise source $\widetilde{e_q}$ is validated for a wide range of applications as the sum of a uniform-distributed noise and a gaussian noise

$$\widetilde{e_q} = \upsilon(\beta \times e_u + (1-\beta) \times e_n) \tag{8}$$

where e_u and e_n are uniform-distributed noise and gaussian noise with variance of 1, υ controls the variance (power) of the global noise and $\beta \in [0,1]$ is a weight allowing the combination of two models. If there is a dominant quantization noise source, the output noise is fairly a uniform distribution and $\beta \approx 1$. In the other extremity, where each noise source contributes the same, $\beta \approx 0$. This model is valid for every systems based on arithmetic operations and using rounding quantization mode.

Computation accuracy evaluation To compute the power expression of the output quantization noise, the technique presented in [7] is used. Given that the code and the channel complex amplitude are constant for a frame, the system can be assumed to be linear and time invariant. For the choice of the code and the channel complex amplitude, the worst case which leads to the maximal quantization noise power is considered. The output quantization noise is a weighted sum of each noise source variance $\sigma^2_{q_i}$:

$$P_e = \sigma_q^2 = \sum_i K_i \sigma^2_{e_i} \tag{9}$$

with K_i, the gain between the output and the noise source. The variance $\sigma^2_{e_i}$ of each noise source is obtained from the quantization step q_i (the least significant bit weight) obtained after quantization:

$$\sigma^2_{e_i} = \frac{q^2}{12} \tag{10}$$

Constraint determination In this part, the expression of the bit error rate BER_{P_e} according to the output quantization noise power P_e is presented. This expression allows determining the maximum quantization noise power satisfied (7). Firstly, the case of a gaussian distribution for the output quantization noise is considered ($\beta = 0$). Inside the system, multiple rounding quantization noises $e_1, e_2, ..., e_K$ are generated. If there is no dominant noise source, due to the central limit theorem, the sum of these noises is then considered gaussian and has the following probability density function (pdf):

$$f_q(x) = \frac{1}{\sigma_q\sqrt{2\pi}} \exp \frac{-x^2}{2\sigma_q^2} \tag{11}$$

In a WCDMA receiver, the thermal noise and multiple access interference (MAI) can be modeled as a gaussian noise source if the transmission channel is additive white Gaussian noise (AWGN) and there is no dominant interferers [9]. In other cases, improved gaussian approximation or alternative method must be used. For simplicity, at first, the received signal is assumed to have two components corresponding to the desired signal and the gaussian noise and interference. Thus, the output is the sum of the output quantization noise e_q and the output receiver noise n_{out}. The expression of the total noise probability density function $f_n(x)$ is as follows:

$$f_n(x) = \frac{1}{\sqrt{\sigma^2_{n_{out}} + \sigma_q^2}\sqrt{2\pi}} \exp \frac{-x^2}{2(\sigma^2_{n_{out}} + \sigma_q^2)} \tag{12}$$

and the following probability distribution function $F_n(x)$:

$$F_n(x) = \frac{1}{2}\left(1 + \mathrm{erf}\,\frac{x}{\sqrt{\sigma^2_{n_{out}} + \sigma_q^2}\sqrt{2}}\right) \tag{13}$$

Since WCDMA uses BPSK/bi-orthogonal transmission, bit error rate can be calculated as follow:

$$\begin{aligned}\mathrm{BER}(\sigma_q, \sigma_{n_{out}}) &= 1 - F_n(1) = \frac{1}{2}\,\mathrm{erfc}\,\frac{1}{\sqrt{\sigma^2_{n_{out}} + \sigma_q^2}\sqrt{2}} \\ &= Q\left(\frac{1}{\sqrt{\sigma^2_{n_{out}} + \sigma_q^2}}\right)\end{aligned} \tag{14}$$

From (7) and (14), the condition for σ_q^2 is:

$$\begin{aligned}\sigma_q^2 &\leq \frac{1}{2}\mathrm{erfc}^{-1}\left((1+\varepsilon)\,\mathrm{erfc}\,\frac{1}{\sigma_{n_{out}}\sqrt{2}}\right)^{-2} - \sigma^2_{n_{out}} \\ &= Q^{-1}\left((1+\varepsilon)Q\left(\sigma_{n_{out}}^{-1}\right)\right)^{-2} - \sigma^2_{n_{out}}\end{aligned} \tag{15}$$

Secondly, the case with a dominant quantization noise has been considered ($\beta = 1$). In this case, the noise distribution is uniform and its pdf $f_q(x)$ is then as follows:

$$f_q(x) = \frac{1}{q}\mathbf{Id}_{[\frac{-q}{2},\frac{q}{2}]} \tag{16}$$

Thus the global noise, including the gaussian noise source with pdf f_c, has the following pdf:

$$f_n(x) = f_c * f_q(x) = \int_{-\infty}^{\infty} f_c(t) f_q(x-t)dt \tag{17}$$

$$= \frac{1}{2q}\left(\text{erf}\frac{x+\frac{q}{2}}{\sqrt{N_0}} - \text{erf}\frac{x-\frac{q}{2}}{\sqrt{N_0}}\right) \tag{18}$$

and the following pdf:

$$F_n(x) = \int_{-\infty}^{x} \frac{1}{2q}(\text{erf}\frac{t+\frac{q}{2}}{\sqrt{N_0}} - \text{erf}\frac{t-\frac{q}{2}}{\sqrt{N_0}}) \tag{19}$$

In case of BPSK, the bit error probability is:

$$\text{BER}(\sigma_q, \sigma_{n_{out}}) = 1 - F_n(1) \tag{20}$$

By the similar way, the precision can be deduced from (7) and (20). Since there is no simple mathematical expression, the criterion is solved numerically.

The accuracy constraint has been determined for different signal-to-noise ratio. The results are presented in Figure 4. The line $P_{s_{out}}$ and $P_{n_{out}}$ correspond to the desired signal s_{out} (symbol) power and the output noise n_{out} power respectively. The difference between the lines $P_{s_{out}}$ and $P_{n_{out}}$ corresponds to the output signal-to-noise ratio. The difference between the lines $P_{s_{out}}$ and P_{e_q} corresponds to the output signal-to-quantization noise ratio (SQNR).

The results show that the SQNR must be increased in order to keep the BER decreasing when the SNR increases. In such case, more accuracy is required to reduce the decision errors due to finite precision arithmetic.

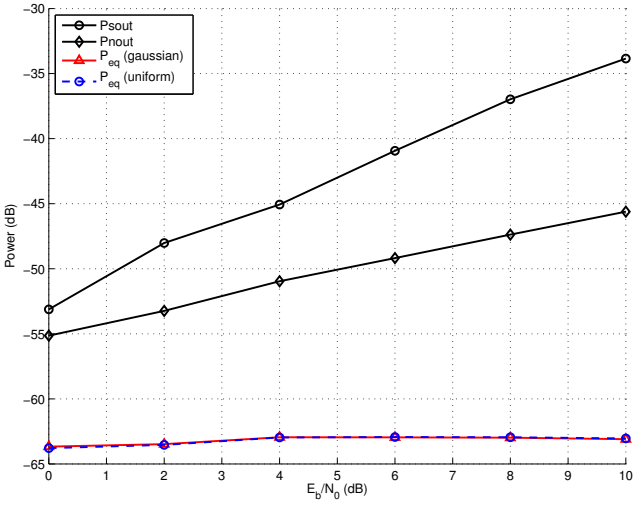

Figure 4: Signal and noise power levels according to the SNR

4.2.2 *Word-length optimization*

The optimization process presented in equation (1) is carried-out with the accuracy constraint defined in equation (15). The optimized word-lengths obtained for different SNR values are presented in Table 1. The results show that the optimized word-lengths vary according to the SNR. Between, 0 dB and 20 dB the word-lengths of the variables *acc* and s_{out} increase respectively by 80% and 66%. Optimization results show that, for a SNR varying from 0 dB to 20 dB, potentially, up to 40% of energy consumption can be saved if the fixed-point specification is adapted according to the SNR.

Table 1: Optimized Rake receiver word-lengths obtained for different SNR values

E_b/N_0 (dB)	1	3	5	7	9	11	13	15	17	19	21
acc	5	6	6	6	7	7	7	7	9	9	9
s_{out}	6	7	7	7	8	9	9	9	9	9	10

5. PATH SEACHER

In this section the results obtained for the path searcher are presented.

5.1 Range estimation

The previous approach is used to estimate the dynamic range of the path searcher described in Figure 2. The input data RX is normalized into $[-1,1]$. It is then multiplied with complex conjugate spreading code $C_{ch}C_G^*$ and results in the interval $[-2,2]$ for each real and imaginary part. For the accumulation along with L (OVSF code length) symbols only the signal is summed up significantly. Thus, the dynamic range is equal to

$$\max(|x_{acc}|) = \frac{2L}{1+3\sigma} \tag{21}$$

The dynamic range of x_{pow} corresponding to the profile power is equal to

$$\max(|x_{pow}|) = \frac{8}{(1+3\sigma)^2} \tag{22}$$

The estimated and simulation based dynamic range of each value is presented in Figure 5. It is noteworthy that estimated and simulated results differ of 1 or 2 bits.

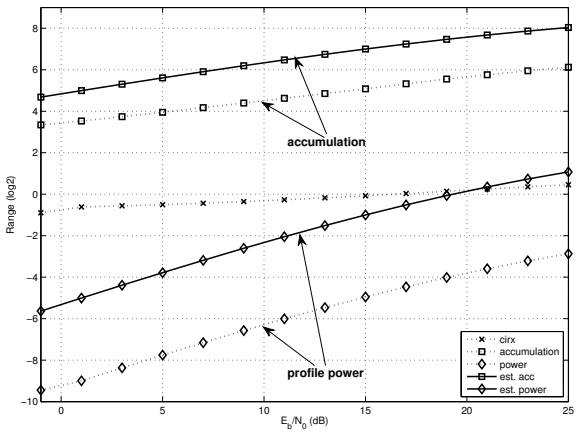

Figure 5: Estimated and simulation based values of range for the path searcher.

5.2 Precision evaluation

The path searcher module cannot use criteria presented in 4.2. This module is based on the detection theory and classical criteria are

Table 2: Optimized searcher word-lengths obtained for different SNR values

E_b/N_0 (dB)	1	3	5	7	9	11	13	15	17	19	21
x_{CM}	8	8	8	8	8	8	8	8	9	9	9
x_{acc}	11	11	11	11	12	12	12	13	13	13	13
x_{pow}	7	6	7	7	8	9	9	10	10	11	11

used to analyze the performance. The *misdetections* (MD) corresponding to the non-detection of an existing path and the *false alarms* (FA) corresponding to the detection of a non-existing path are both measured.

To analyze the path searcher performance, the multi-path Rayleigh channel is considered. The output of the path searcher before decision x_{pow} is made up of three components corresponding to the signal s_{pow}, the receiver noise n_{pow} and the output quantization noise e_q. Compared to the Rake receiver, the distribution of the output signal is not straight. Two cases have to be considered. When there is a path, the output value depends on the module of the complex amplitude α_i associated to i^{th} path. Without path, the output values depend on the code properties. In this last case, the modeling of the output signal distribution is complex. Thus the technique based on simulation presented in [8] has been retained to determine the accuracy constraint and a Monte Carlo method is used to measure the FA and MD values. A Rayleigh channel model respecting the 3GPP channel case 3 [1] without Doppler effect is used, corresponding to a multi-path fading with four path components (gain, delay): (0 dB, 0 ns); (-3 dB, 261 ns); (-6 dB, 521 ns); (-9 dB, 781 ns).

The evolution of the false alarm according to the SNR are presented in Figure 6 for different output quantization noise levels. The false alarms are more sensitive to the quantization noise than the misdetections. For the same quantization noise level, the mean of misdetected paths does not evolve and is very closed to the one in infinite precision. Hence, the accuracy constraint is determined from the false alarm criteria, then the data word-lengths are optimized. The results are presented in Table 2. The path searcher word-lengths, as same as the Rake receiver, depend on the SNR values.

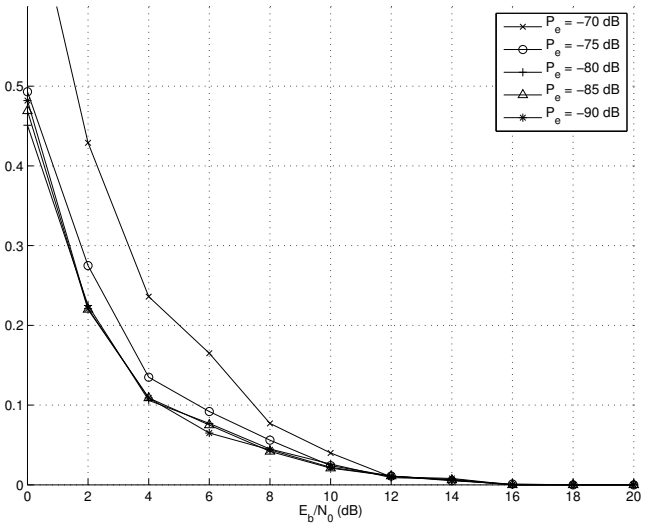

Figure 6: Mean of non-valid detected paths (false alarms) obtained for different SNR values

6. CONCLUSION

For the embedded wireless system design, the arithmetic optimization aspect is one of the ways to reduce the implementation cost and the power consumption. An approach has been proposed to optimize the fixed-point specification according to the required application performances. A new approach has been proposed to estimate more accurately the data dynamic range by exploiting the application properties. The accuracy constraint has been determined from the required application performances. For the bit error rate, the analytical expression of the accuracy constraint according to the BER has been proposed. The results show that the fixed-point specification depends on the input SNR. An approach in which the fixed-point specification is adapted dynamically according to the input receiver SNR can be investigated. In the case of low SNR, lower word-length data can be used and energy can be saved.

REFERENCES

[1] 3GPP. TS 25.104 V8.3.0: Base Station radio transmission and reception (FDD), 2008.

[2] B. Evans. Modem Design, Implementation, and Testing Using NI's LabVIEW. In *National Instrument Academic Day*, Beirut, Lebanon, June 2005.

[3] J. Eyre and J. Bier. The evolution of DSP processors. *IEEE Signal Processing Magazine*, 17(2):43–51, March 2000.

[4] K. Han, I. Eo, K. Kim, and H. Cho. Numerical word-length optimization for CDMA demodulator. In *Proc. 2001 IEEE International Symposium on Circuits and Systems (ISCAS'01)*, volume 4, pages 290–293, 2001.

[5] N. Herve, D. Menard, and O. Sentieys. Data wordlength optimization for FPGA synthesis. *IEEE Workshop on Signal Processing Systems (SiPS'05)*, pages 623–628, 2005.

[6] R. Kearfott. Interval computations: Introduction, uses, and resources. *Euromath Bulletin*, 2(1):95–112, 1996.

[7] D. Menard, R. Rocher, and O. Sentieys. Analytical Fixed-Point Accuracy Evaluation in Linear Time-Invariant Systems. *IEEE Trans. Circuits Syst. I*, 55(10):3197–3208, Nov. 2008.

[8] D. Menard, R. Rocher, O. Sentieys, and O. Serizel. Accuracy Constraint Determination in Fixed-Point System Design. *EURASIP Journal on Embedded Systems*, 2008(Article ID 242584), 2008.

[9] M. Pursley. Performance Evaluation for Phase-Coded Spread-Spectrum Multiple-Access Communication–Part I: System Analysis. *IEEE Trans. Commun. [legacy, pre-1988]*, 25(8):795–799, 1977.

[10] C. Sengupta, S. Das, J. R. Cavallaro, and B. Aazhang. Fixed point error analysis of multiuser detection and synchronization algorithms for CDMA communication systems. In *Proc. 1998 IEEE International Conference on Acoustics, Speech, and Signal Processing (ICASSP'98)*, pages 3249–3252, 1998.

[11] W. Strauss. DSP chips take on many forms. DSP-FPGA.com Magazine, March 2006.

[12] W. Strauss. Hanging up on analog and flexing Wireless/DSP muscles. Technical report, Forward Concepts, 2008.

[13] K. Tachikawa. *W-CDMA Mobile Communications System*. Wiley, 2002.

[14] H. Zhao, T. Ottosson, E. Strom, and A. Kidiyarova-Shevchenko. Performance analysis of a fixed-point successive interference canceller for WCDMA. In *Proc. 60th IEEE Vehicular Technology Conference (VTC'04-Fall)*, volume 3, pages 1919–1923, Sept. 2004.